AD NUMBER

AD-855 156

CLASSIFICATION CHANGES

TO **UNCLASSIFIED**

FROM **NEVER CLASSIFIED**

AUTHORITY

U.S. Army Materiel Command, Washington, DC; June 1969.

AD NUMBER

AD-855 156

NEW LIMITATION CHANGE

TO **DISTRIBUTION STATEMENT - A**

Approved for Public Release; Distribution Unlimited.

LIMITATION CODE - 1

FROM **DISTRIBUTION STATEMENT - NONE**

No Prior DoD Distribution Security Control Statement.

AUTHORITY

Army Ballistic Research Lab., via ltr. dtd April 22, 1981.

REPRODUCTION QUALITY NOTICE

This document is the best quality available. The copy furnished to DTIC contained pages that may have the following quality problems:

- Pages smaller or larger than normal.
- Pages with background color or light colored printing.
- Pages with small type or poor printing; and or
- Pages with continuous tone material or color photographs.

Due to various output media available these conditions may or may not cause poor legibility in the microfiche or hardcopy output you receive.

☐ If this block is checked, the copy furnished to DTIC contained pages with color printing, that when reproduced in Black and White, may change detail of the original copy.

BRL MR 1983

BRL

AD

MEMORANDUM REPORT NO. 1983

AN EXPERIMENTAL INVESTIGATION AT SUPERSONIC MACH NUMBERS OF BASE DRAG OF VARIOUS BOATTAIL SHAPES WITH SIMULATED BASE ROCKET EXHAUST

by

Joseph Huerta

June 1969

U.S. ARMY ABERDEEN RESEARCH AND DEVELOPMENT CENTER
BALLISTIC RESEARCH LABORATORIES
ABERDEEN PROVING GROUND, MARYLAND

BALLISTIC RESEARCH LABORATORIES

MEMORANDUM REPORT NO. 1983

JUNE 1969

AN EXPERIMENTAL INVESTIGATION AT SUPERSONIC MACH NUMBERS OF BASE DRAG OF VARIOUS BOATTAIL SHAPES WITH SIMULATED BASE ROCKET EXHAUST

Joseph Huerta

Exterior Ballistics Laboratory

RDT&E Project No. 1T061102A33D

ABERDEEN PROVING GROUND, MARYLAND

BALLISTIC RESEARCH LABORATORIES

MEMORANDUM REPORT NO. 1983

JHuerta/lca
Aberdeen Proving Ground, Md.
June 1969

AN EXPERIMENTAL INVESTIGATION AT SUPERSONIC MACH NUMBERS OF BASE DRAG OF VARIOUS BOATTAIL SHAPES WITH SIMULATED BASE ROCKET EXHAUST

ABSTRACT

An experimental investigation was conducted to determine the effect of boattail geometry and simulated base rocket nozzle flow on overall base drag. All tests were performed at Mach numbers 2.50, 3.00 and 3.50. Reasonable prediction of base drag for the reported boattail shapes can be made by using approximate and empirical equations. A conical boattail produced less drag than the other boattail shapes investigated. The maximum nozzle stagnation to free-stream pressure ratio reported is 315.

TABLE OF CONTENTS

		Page
	ABSTRACT	3
	LIST OF ILLUSTRATIONS	7
	LIST OF SYMBOLS	9
I.	INTRODUCTION	11
II.	APPARATUS	11
	A. Wind Tunnel	11
	B. Test Model	12
	C. Instrumentation	12
III.	TEST PROCEDURE AND CONDITIONS	13
IV.	DATA REDUCTION	14
V.	DISCUSSION OF THEORETICAL AND EMPIRICAL CALCULATIONS	14
VI.	PRESENTATION AND DISCUSSION OF DATA	17
VII.	CONCLUSIONS	19
	REFERENCES	43
	DISTRIBUTION LIST	45

LIST OF ILLUSTRATIONS

Figure		Page
1.	Typical Model Installation in the Wind Tunnel	20
2.	Model Dimensions and Boattail Tap Locations	21
3.	Close Up of Model Pressure Taps	22
4.	Boattail Configurations	23
5.	Boattail Dimensions and Base Tap Locations	24
6.	Pressure Scanner System	25
7.	Boattail Pressure Distribution	26
8.	Effect of Sustainer Nozzle Operating Pressure on Boattail Drag	31
9.	Effect of Mach Number on Boattail Drag	32
10.	Effect of Sustainer Nozzle Operating Pressure on Base Pressure	33
11.	Effect of Sustainer Nozzle Operating Pressure on Base Drag	36
12.	Effect of Jet Mass Flow on Base Drag	39
13.	Effect of Sustainer Nozzle Operating Pressure on Total Drag	41
14.	Schlieren Photographs of Base Flow Field for Boattail No. 6	42

LIST OF SYMBOLS

a_j^*	sonic velocity at jet exit conditions
m_i	mass flow based on A_B and free stream conditions
m_j	mass flow through sustainer nozzle
p_b	average base pressure
p_c	sustainer nozzle stagnation pressure
p_j	jet exit static pressure
p_ℓ	local static pressure
p_∞	free-stream static pressure
p_2	static pressure downstream of a corner
q	free-stream dynamic pressure
r	radius of body at point x
s	rectangular coordinate in streamline direction
x	coordinate measured from vertex of body
x_2	position of a corner
A_B	maximum body area
A_b	base area
A_j	jet exit area
A_ℓ	increment of area associated with the local static pressure
C_{DB}	base drag coefficient
C_{DBT}	boattail drag coefficient
C_l	characteristic coordinate along Mach line
D_b	base diameter
D_j	jet exit diameter
M	Mach number

LIST OF SYMBOLS (Continued)

M_j	jet exit Mach number
M_j^*	dimensionless jet velocity, V_j/a_j^*
M_∞	free-stream Mach number
P_o	tunnel stagnation pressure
Re	free-stream Reynolds number
V_j	jet exit velocity
V_ℓ	local velocity
γ	ratio of specific heats
δ	flow deflection angle
δ_1	flow deflection angle before a corner
δ_2	flow deflection angle after a corner
μ	Mach angle (arcsin 1/M)

I. INTRODUCTION

Methods for reducing missile drag, especially base drag, have been of considerable practical importance. As a consequence, the Army Missile Command (MICOM), Redstone Arsenal, Alabama, has been conducting a continual program to investigate techniques for minimizing missile base drag. As a part of this continuing investigation, the present tests were conducted in the supersonic wind tunnel of the Ballistic Research Laboratories (BRL) to determine the effect of six boattail configurations on drag. Base drag was measured in the presence of a sustainer rocket motor exhausting cold flow through the base. A comparison of experimental data and a second-order shock-expansion method for boattail-pressure distribution was made. An empirical technique was employed to estimate "power on" base drag and these results are compared with measured data.

The basic model was a strut-mounted body of revolution. The section forward of the boattail consisted of a tangent-ogive nose followed by a cylindrical center body. Pressure data were obtained along the boattail surface and model base at nominal test Mach numbers of 2.50, 3.00 and 3.50 for each boattail shape with the model at zero angle of attack. Sustainer nozzle pressure was also varied for each boattail. The ratio of nozzle exit diameter to body diameter was 0.200 and the nozzle exit Mach number was 2.7 for fully developed flow or "power on" condition.

II. APPARATUS

A. Wind Tunnel

Supersonic Wind Tunnel No. 1 of the Ballistic Research Laboratories was used to acquire the data. This is a two-dimensional continuously operated, variable density, closed circuit tunnel having a test section 15 inches high and 13 inches wide. Two flexible steel plates form the upper and lower walls of the nozzle section. A complete description of this facility and its flow characteristics are given in References 1 and 2.

B. Test Model

The model was a body of revolution attached to the upper test section wall by a swept back support strut at zero angle of attack. It consisted of a tangent-ogive nose attached to a cylindrical center body and ending with a boattail. Figure 1 shows a photograph of the model installation in the test section and the schematic of Figure 2 presents the pertinent dimensions of the model and support strut. The overall length of the model was 15.0 inches and the diameter was 2.500 inches. The support strut was a modified double wedge section, 0.435 inch thick with a 3.125 inches chord. The exit diameter of the sustainer nozzle was 0.500 inch or 0.200 calibers and the exit Mach number was 2.7. Model pressure taps were placed opposite the model support strut and located on the cylindrical surface, boattail surface and at the base. The photograph of Figure 3 presents a view of these pressure taps.

Six boattail configurations were investigated in this program. All of these boattails were one caliber in length. Figures 4 and 5 define the geometric shapes of these boattails which consisted of conical, concave, convex and reverse curvature configurations.

C. Instrumentation

The model pressures were transmitted through metal tubing to a pressure scanner system. The pressure scanner (Figure 6) is a solid metal block which is channeled such that, with the aid of pneumatically operated valves, seals and stepping switches, pressures can be measured in sets of seven pressures per cycle. This scanner unit is necessary since the tunnel automatic data acquisition system is capable of handling only eight inputs per sampling time. Pressures from the scanner were measured by a group of pressure transducers of suitable pressure range. The electrical output signals from these transducers were converted by an automatic readout system to digital readings which were recorded automatically by typewriter. A complete description of the scanner is given in Reference 3.

The sustainer nozzle total pressure and tunnel total pressure were monitored continuously throughout the period of data acquisition. The sustainer nozzle stagnation pressure was measured in its plenum chamber.

A schlieren system with camera provides continuous visual indication, as well as photographs, of the flow conditions in the test section.

III. TEST PROCEDURE AND CONDITIONS

The flow in the wind tunnel was established at a low stagnation pressure and then the pressure was raised to the desired level. The sustainer nozzle pressure was adjusted to the proper value. With all flow conditions at steady state, model pressure readings were obtained with the pressure scanner system. Before each set of model pressures were recorded, it was ascertained that these pressures were stabilized in the scanner system by observing their respective dial readings on the control panel. Pressure readings were recorded when all dial motion ceased. After making a complete pressure sampling cycle, the jet pressure was adjusted to the next value, and the model pressure reading cycle was repeated. The available line pressure for the sustainer nozzle was 300 psia. The variation in tunnel stagnation and sustainer nozzle pressure was less than 0.1 percent.

The average tunnel operating conditions are listed in Table I for the three Mach numbers. The specific humidity was maintained below 0.0002 pound of water per pound of air. Schlieren photographs were taken of the flow field for selected model configurations.

Table I. Tunnel Operation Conditions

Mach No.	P_o psia	q psi	Re x 10^{-6} per inch
2.50	28.88	7.40	0.50
3.00	40.45	6.94	0.50
3.50	52.69	5.92	0.50

A narrow band of fine grit was placed on the nose surface near the tip to insure a turbulent boundary layer at all times.

IV. DATA REDUCTION

The raw pressure data were converted into the required ratio and coefficient form by a computer. The data acquisition system automatically recorded the raw data from the pressure transducers in digital typewritten and coded punched tape form. The punched tape was used to obtain punched cards which were fed into the computer for reduction and tabulation of the raw data into the desired form.

The local pressures were weighted by area to determine the boattail and base drag coefficients. The boattail and base drag coefficients were calculated from the following general relationship

$$C_D = \frac{-\sum_{i=1}^{n} [(p_{\ell_i} - p_\infty) A_i]}{q A_B}$$

n = number of local pressures and associated incremental areas

where p_ℓ is the local pressure. The area, A, used to calculate boattail drag is the local area, A_ℓ, projected on the vertical plane. The overall error in determining the model static pressures was approximately ± .003 psi.

V. DISCUSSION OF THEORETICAL AND EMPIRICAL CALCULATIONS

The equation for the streamwise pressure gradient is given as

$$\frac{\partial p}{\partial s} - \frac{2 \gamma p}{\sin 2\mu} \frac{\partial \delta}{\partial s} = \frac{1}{\cos \mu} \frac{\partial p}{\partial C_l}$$

In obtaining the Prandtl-Meyer relation, the pressure is considered constant along the first-family Mach lines. Therefore, the right hand part of the above equation becomes zero and the solution of the integrated equation is the Prandtl-Meyer relation. The second-order shock expansion method imposes a different condition on the pressure gradient equation to obtain an approximate solution (Reference 5).

First consider a body of revolution with a pointed nose and supersonic flow on its surface. Drawing a series of tangent lines to this body contour results in an approximate shape consisting of a series of frustums with a cone vertex. Now on this new geometric shape, it can be assumed that the flow direction does not change within a single element. Now it can be stated that $\partial\delta/\partial s = 0$ and the pressure gradient equation reduces to

$$\frac{\partial p}{\partial s} = \frac{1}{\cos \mu} \frac{\partial p}{\partial C_1}$$

The solution to the above differential equation is the second-order shock expansion method which is

$$p = p_f - (p_f - p_2)\, e^{-\eta}$$

where p_f = pressure on a cone tangent to the body at the same point as a frustum element

$$\eta = \left(\frac{\partial p}{\partial s}\right)_2 \frac{x - x_2}{(p_f - p_2) \cos \delta_2}$$

$$\left(\frac{\partial p}{\partial s}\right)_2 = \frac{B_2}{r} \left(\frac{\Omega_1}{\Omega_2} \sin \delta_1 - \sin \delta_2\right) + \frac{B_2}{B_1} \frac{\Omega_1}{\Omega_2} \left(\frac{\partial p}{\partial s}\right)_1$$

$$B = \frac{\gamma p M^2}{2 (M^2 - 1)} = \frac{q}{M^2 - 1}$$

and

$$\Omega = \frac{1}{M} \left[\frac{1 + \left(\frac{\gamma - 1}{2}\right) M^2}{\frac{\gamma + 1}{2}}\right]^{\frac{\gamma + 1}{2 (\gamma - 1)}}$$

The above equation for Ω is the one dimensional area ratio. Now the second-order equation gives the pressure variation along the surface of the body.

Only the boattail surface pressures are of interest here, so the foregoing second-order equation is further simplified by imposing the following conditions:

1. $(\partial p/\partial s)_1 = 0$
2. $p_f = p_\infty$ or $p_1 = p_\infty$
3. $x = 0$ at the start of the boattail which eliminates the dimension x_2

The following sketch shows that $\delta_1 = 0^\circ$, and δ_2 is a negative angle.

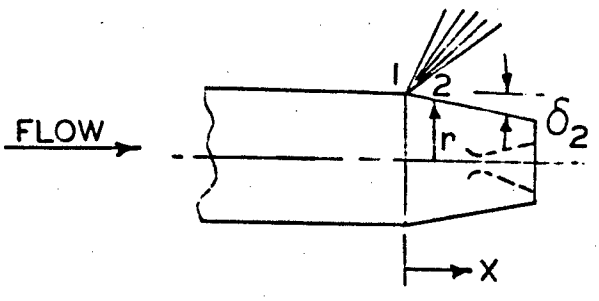

The boattail pressure distributions were calculated from the following set of simplified equations.

$$p = p_\infty - (p_\infty - p_2)\, e^{-\eta}$$

$$\eta = \left(\frac{\partial p}{\partial s}\right)_2 \frac{}{(p_\infty - p_2)\cos \delta_2}$$

$$\left(\frac{\partial p}{\partial s}\right)_2 = -\frac{B_2}{r} \sin \delta_2$$

$$B_2 = \frac{\gamma p_2 M_2^2}{2 (M_2^2 - 1)}$$

The presence of nozzle flow at the base adds to the complexity of the flow mechanism at the base which is difficult to analyze. Consequently, empirical results have been sought by correlation of available experimental data (Reference 6). A reasonable base pressure prediction

for a base with nozzle flow can be made by use of the following empirical equation:

$$\frac{p_b}{p_\infty} = \frac{1}{M_j^*}\left[\frac{3.5}{1 + 2.5\,(A_b/A_B)}\right]\left[0.19 + 1.28\left(\frac{R_{mf}}{1 + R_{mf}}\right)\right]$$

where

$$R_{mf} = \frac{(\dot{m}\,V)_j}{(\dot{m}\,V)_\infty} = \frac{\gamma_j\, p_j\, A_j\, M_j^2}{\gamma_\infty\, p_\infty\, A_B\, M_\infty^2}$$

The base drag coefficient is then calculated by use of the equation:

$$C_{D_B} = \frac{2}{\gamma_\infty\, M_\infty^2}\left(1 - \frac{p_b}{p_\infty}\right)\left(\frac{A_b - A_j}{A_B}\right)$$

VI. PRESENTATION AND DISCUSSION OF DATA

Figures 7 through 9 present data of the boattail portion of all test configurations. The curves in Figures 10, 11 and 12 indicate results of base measurements for these configurations. A comparison of total drag (boattail and base drag) for configurations 6, 7 and 8 is presented in Figure 13. The test data presented are for test Mach numbers of 2.50, 3.00 and 3.50.

The boattail surface pressure distributions were determined for the six boattail configurations and typical distributions are presented in Figure 7 as a function of distance in calibers from the boattail corner. For boattail configurations 6, 7 and 8, there are included, for comparison, pressure distribution curves obtained by the method of characteristics at Mach numbers 2.50 and 3.00 and by the second-order shock expansion method of Reference 5 for all three Mach numbers. Configuration 11 data are presented for Mach numbers 2.50 and 3.00 with the method of characteristic curves included for comparison. Either method appears to predict the pressure distribution of these boattails well for

at least the last two-thirds of the boattail surface. The wide differences between experimental points and the curves at the beginning of the boattail must be due to the boundary layer present at the corner.

The data of Figure 8 provides evidence that the flow from the sustainer nozzle has negligible effect on the boattail drag. The boattail drag coefficient of each boattail configuration appears unchanged for all base flow conditions.

The variation in boattail drag with Mach number is shown in Figure 9. It appears that the conical boattail configuration 6 offers the least drag when compared to other boattail shapes having the same base diameter.

The data of Figure 10 indicate the influence of the base nozzle flow on base pressure for the case of fully developed flow in the nozzle. Results for configurations 6, 7 and 8 are presented. The results of configuration 6 apply to configurations 9, 10 and 11 as well. The method of Reference 6 for predicting base pressure was utilized in calculating the curves shown with these data for comparison. Reasonable predictions of base pressure can be made with this empirical method. However, it appears that the ratio of nozzle diameter to base diameter has a strong influence on accuracy of the prediction. The results in Figure 11 are the base pressure data of Figure 10 reduced to base drag coefficient form and the comments made on Figure 10 data apply to these also. The base drag as a function of the sustainer jet flow parameter is displayed in Figure 12. These curves show that the base drag for configurations 6, 9, 10 and 11 is the same as was pointed out above.

A comparison of total drag (boattail and base drag) for the three conical boattails and a square base configuration from Reference 7 is shown in Figure 13. Only slight differences in total drag are indicated for the conical boattails. However, the square base configuration has about 60 percent more drag than the conical boattail configurations.

The schlieren photographs of Figure 14 show the flow field at the base for configuration 6 at Mach numbers 2.50 and 3.50 for base jet flow off and on.

VII. CONCLUSIONS

From this investigation, it can be concluded that less total drag results from a conical boattail configuration than any of the other contours tested.

Boattail pressure distribution can be determined over at least the last two-thirds of a conical boattail surface using the approximate shock-expansion method of Reference 5 which is much easier to use than the method of characteristics.

A reasonable prediction of base drag with rocket flow at the base can be made using the empirical method of Reference 6.

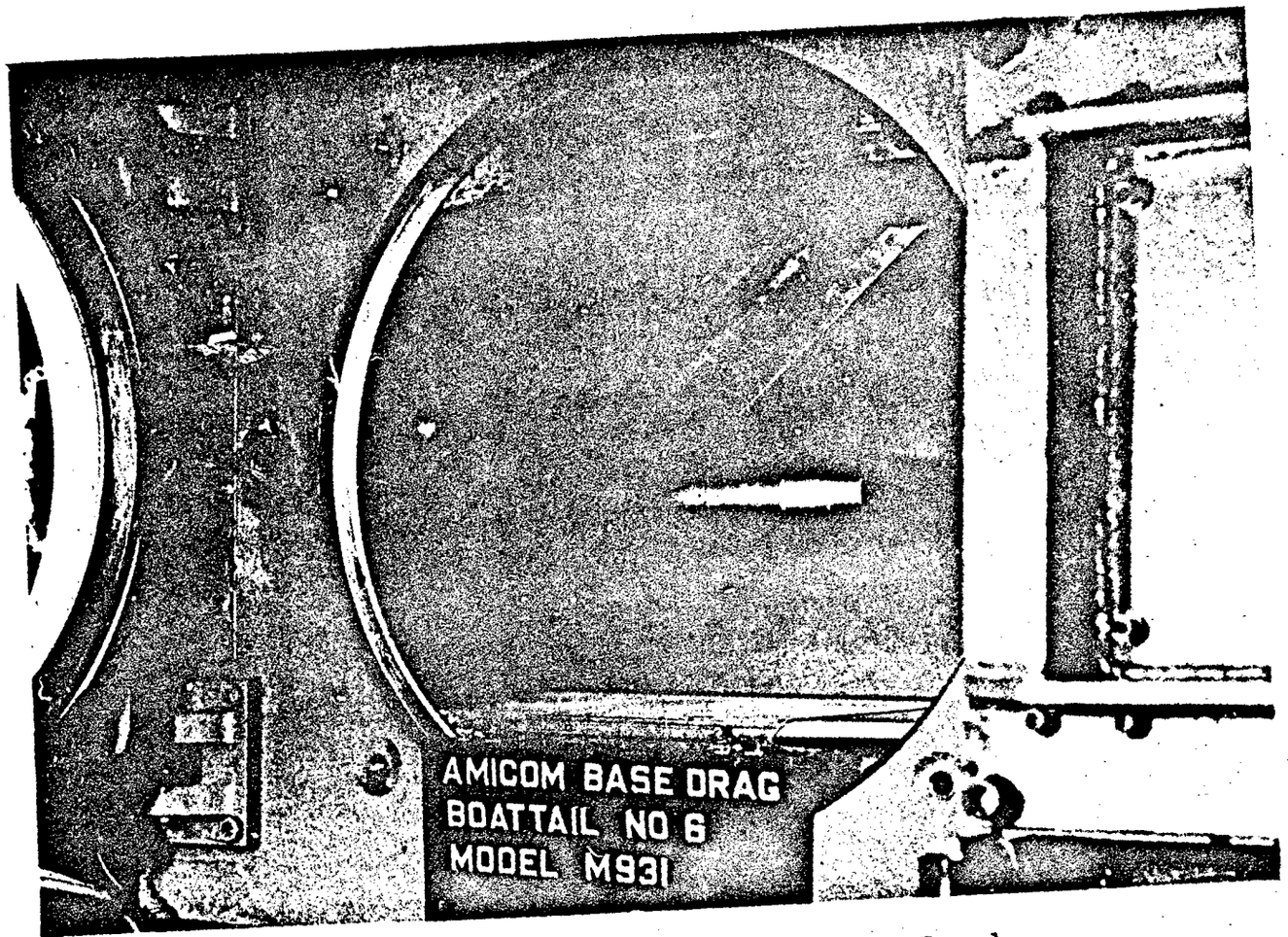

Figure 1. Typical Model Installation in the Wind Tunnel

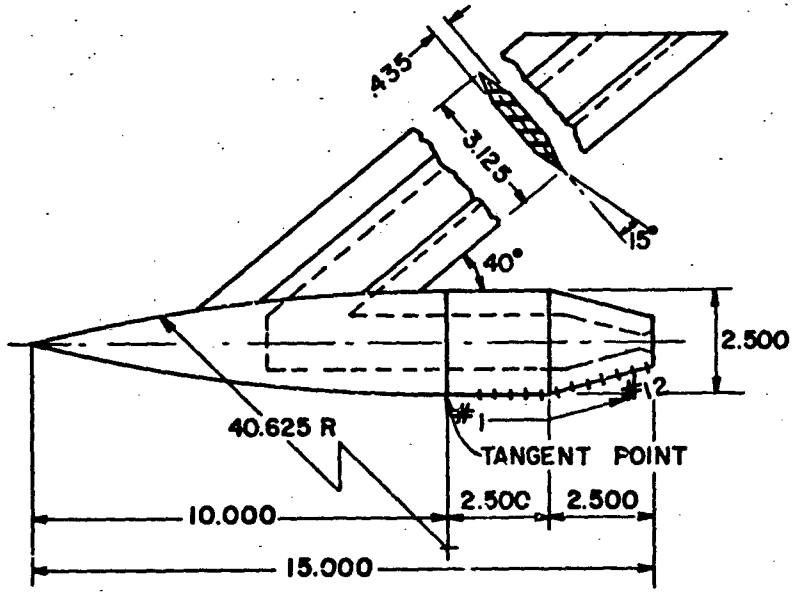

MODEL DIMENSIONS

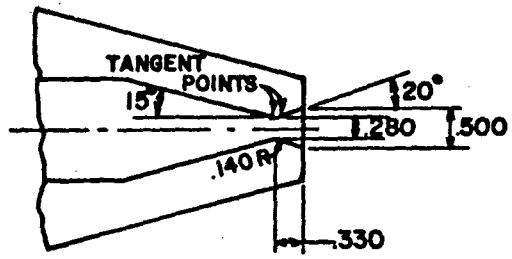

NOZZLE DIMENSIONS

MODEL SURFACE TAP LOCATION	
TAP	DISTANCE FROM BASE
1	3.366
2	2.964
3	2.564
4	2.434
5	2.138
6	1.842
7	1.546
8	1.250
9	0.954
10	0.658
11	0.362
12	0.066

Figure 2. Model Dimensions and Boattail Tap Locations

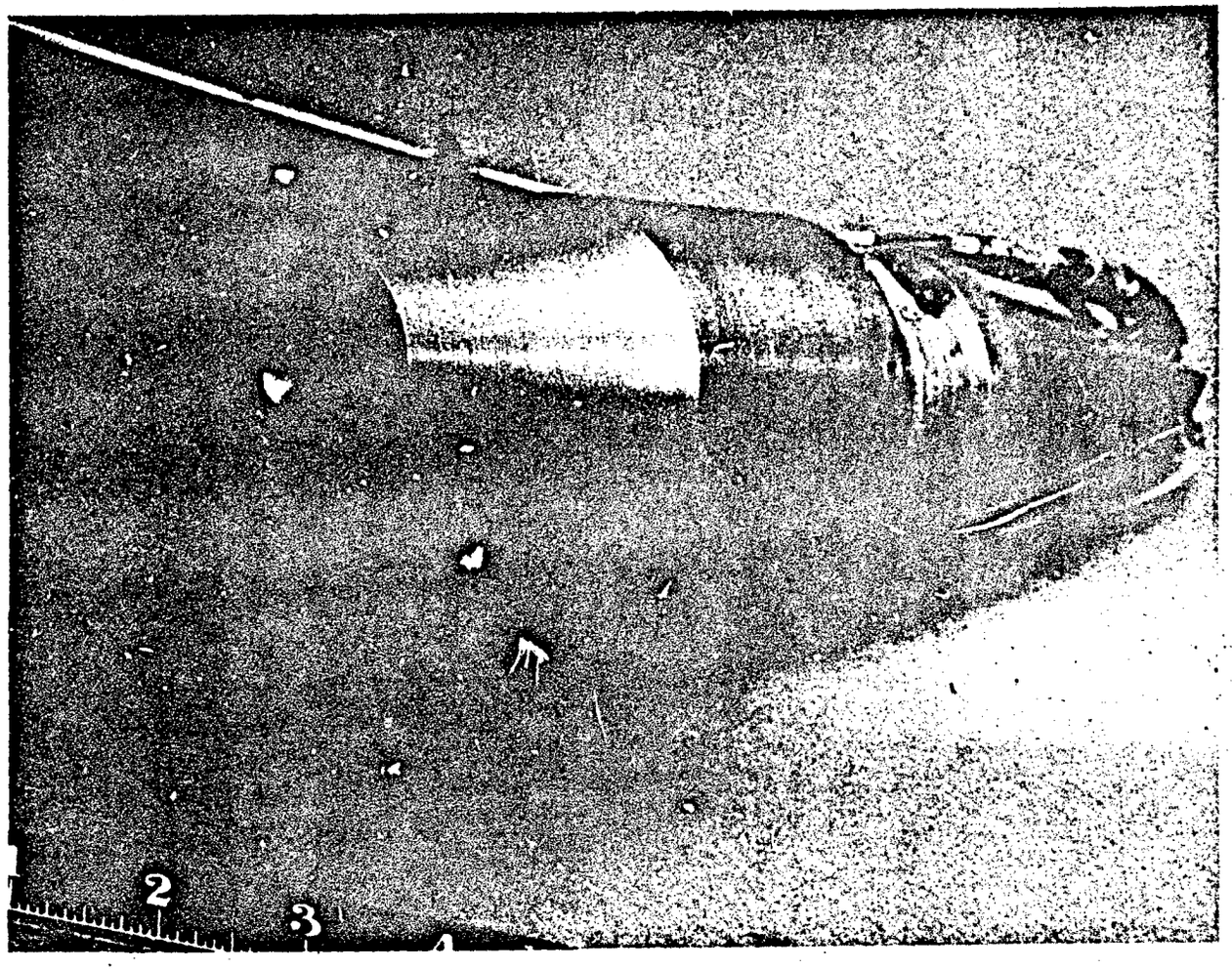

Figure 3. Close Up of Model Pressure Taps

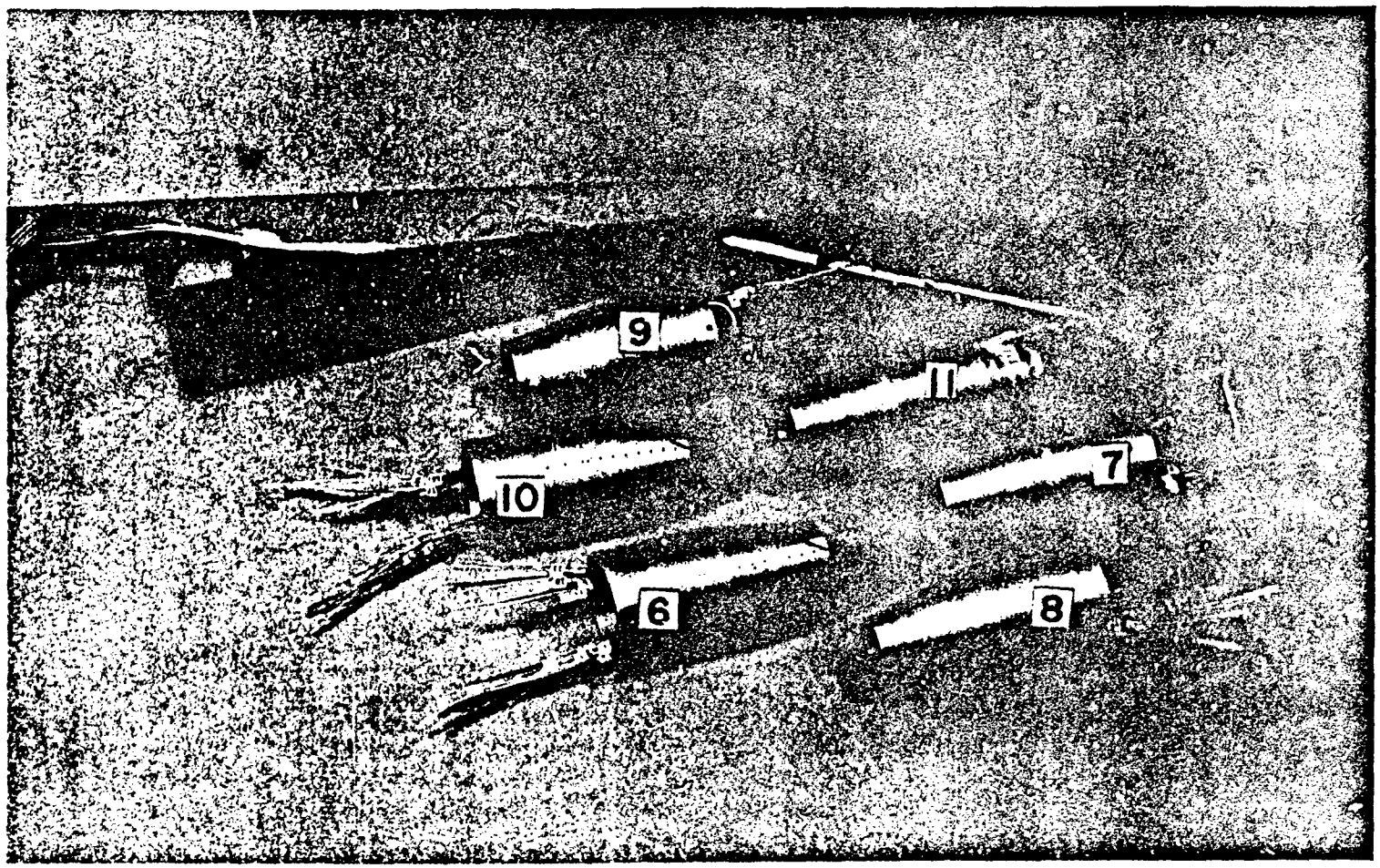

Figure 4. Boattail Configurations

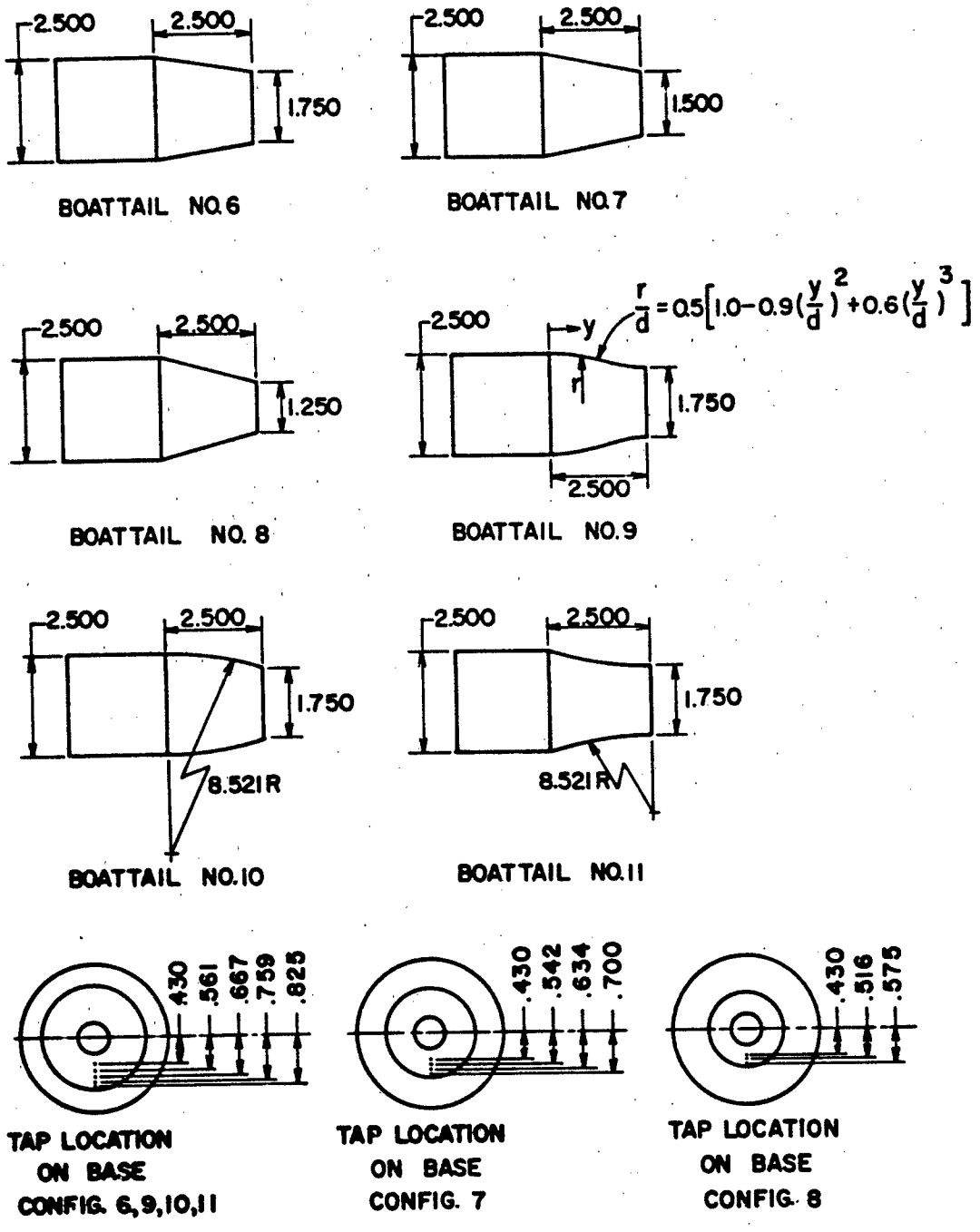

Figure 5. Boattail Dimensions and Base Tap Locations

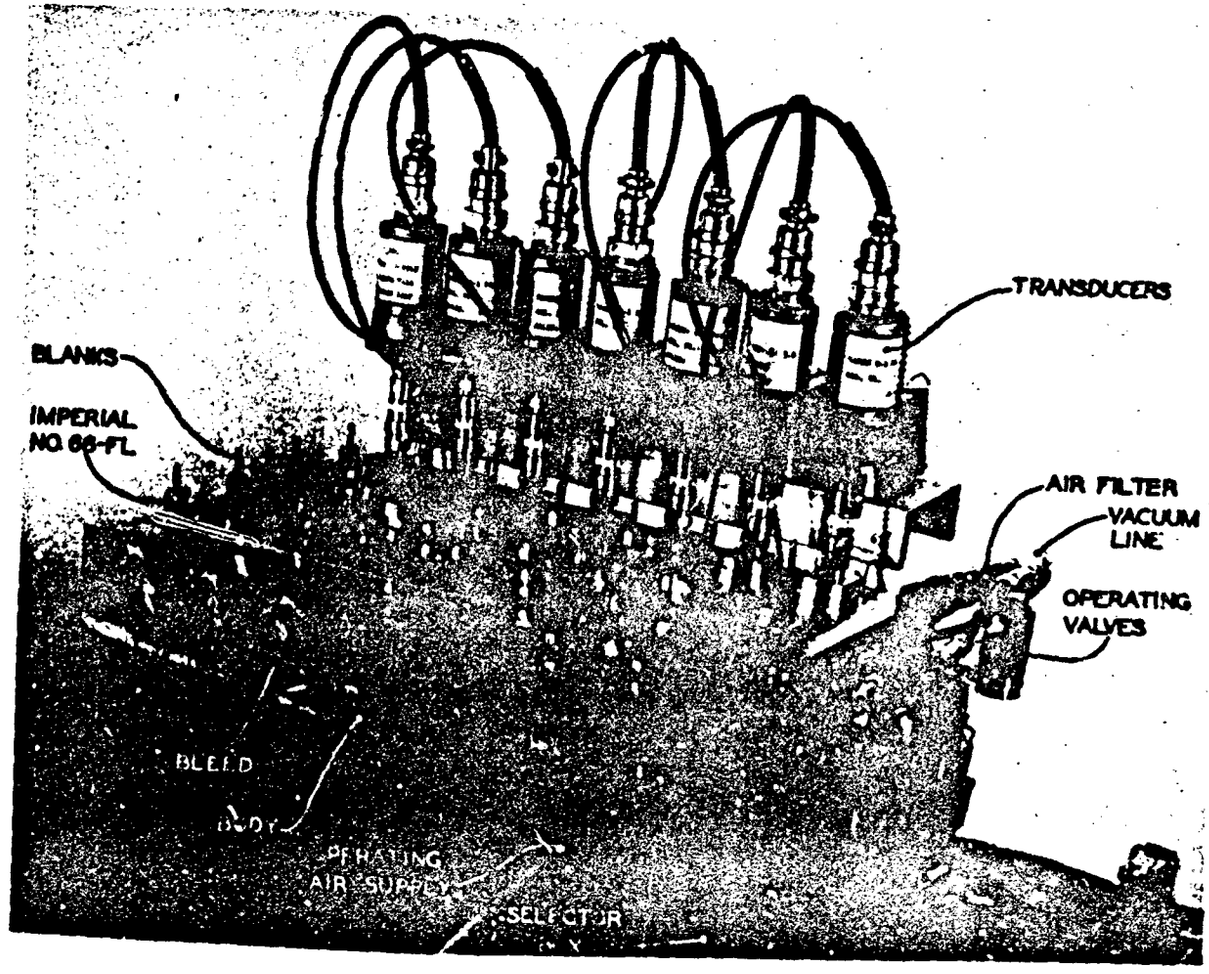

Figure 6. Pressure Scanner System

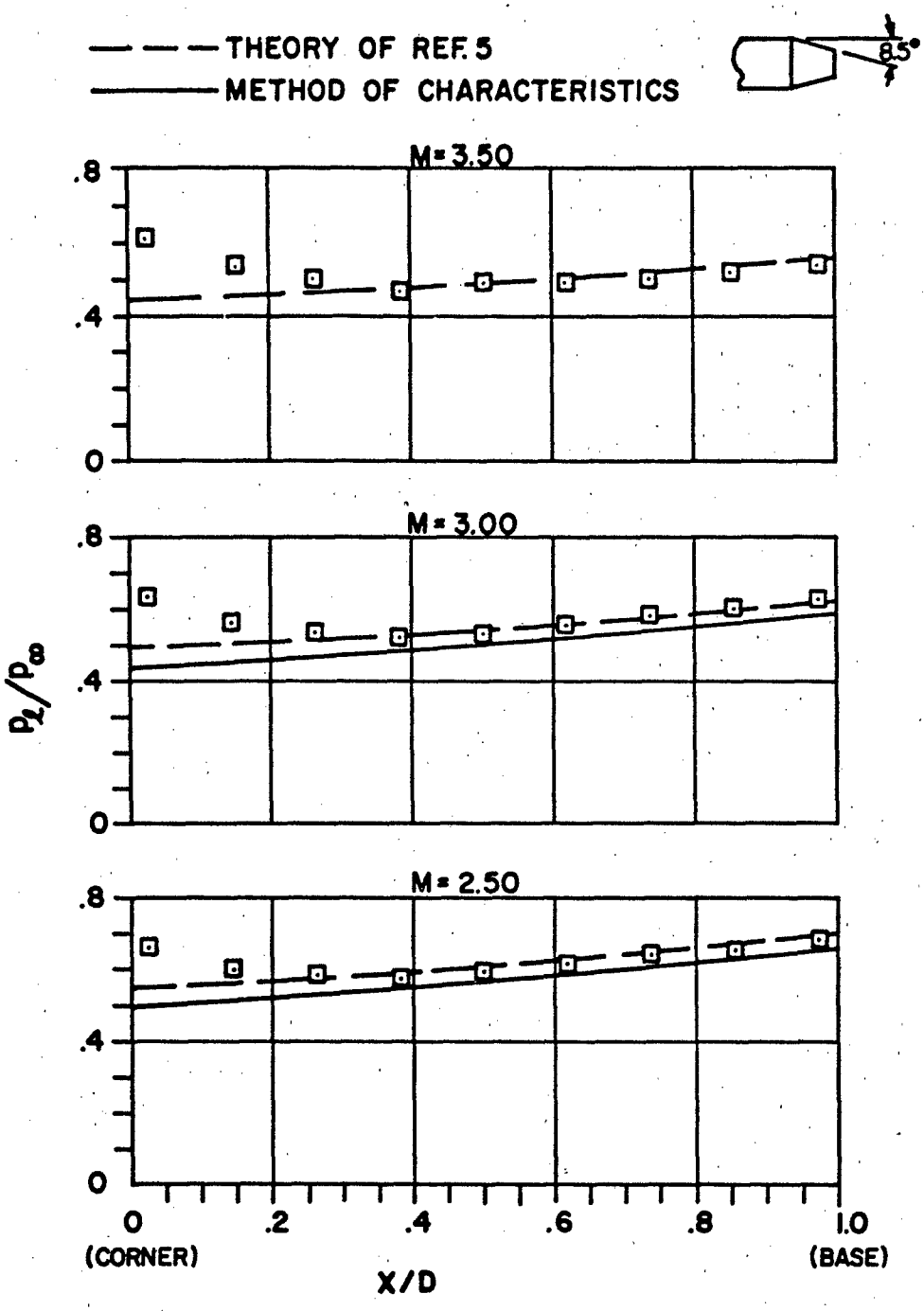

(a) Boattail No. 6

Figure 7. Boattail Pressure Distribution

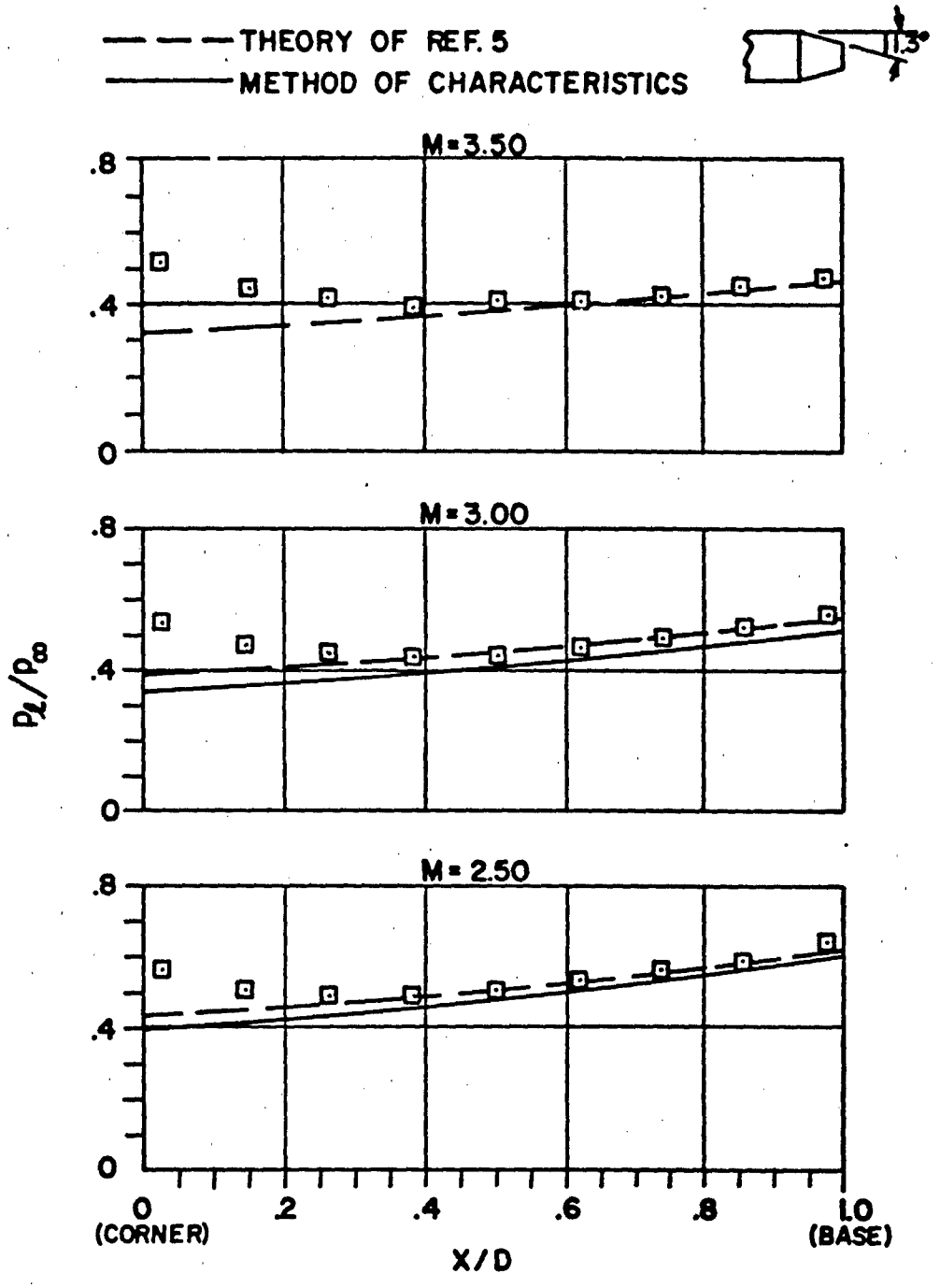

(b) Boattail No. 7

Figure 7. Continued

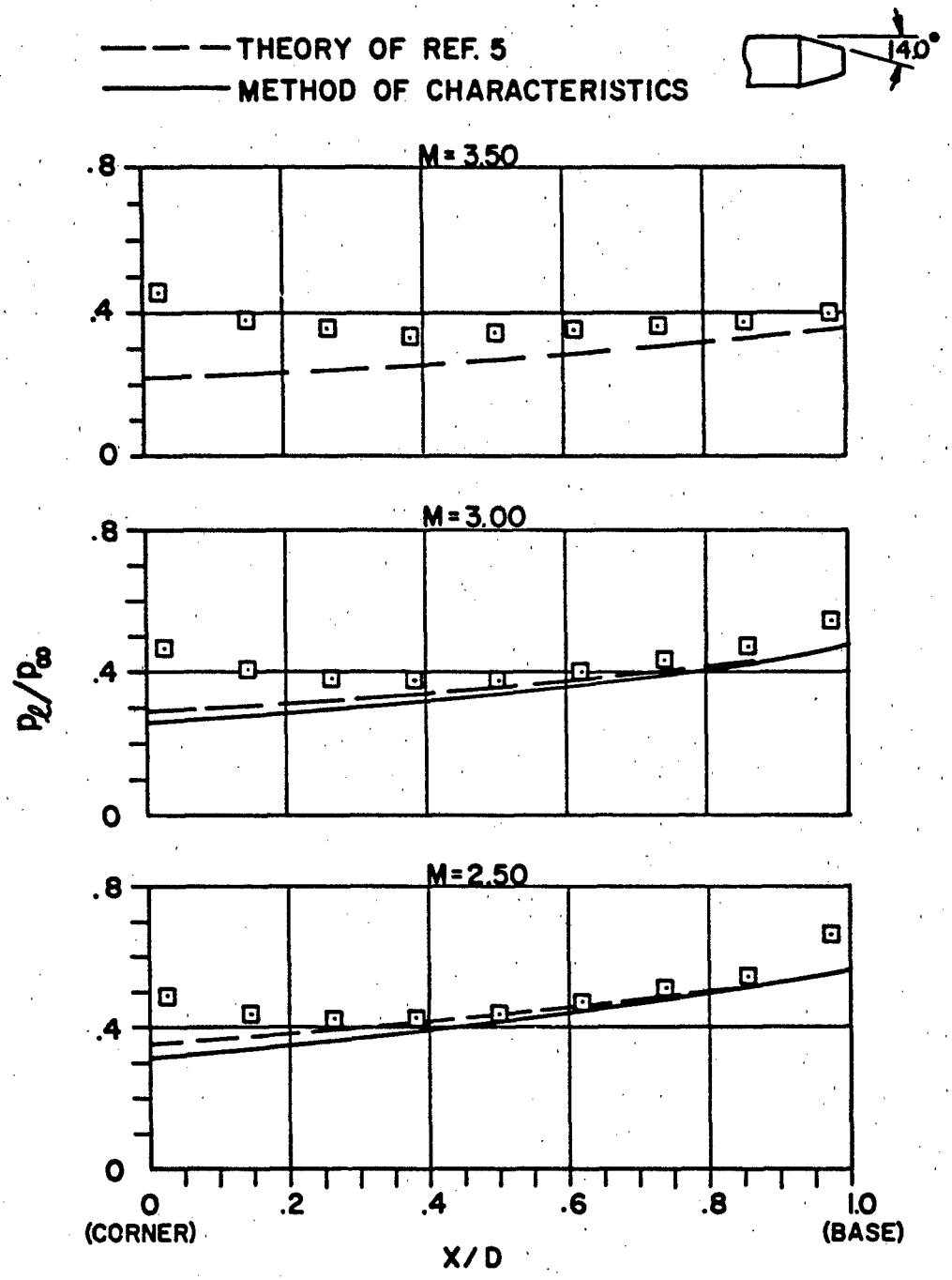

(c) Boattail No. 8

Figure 7. Continued

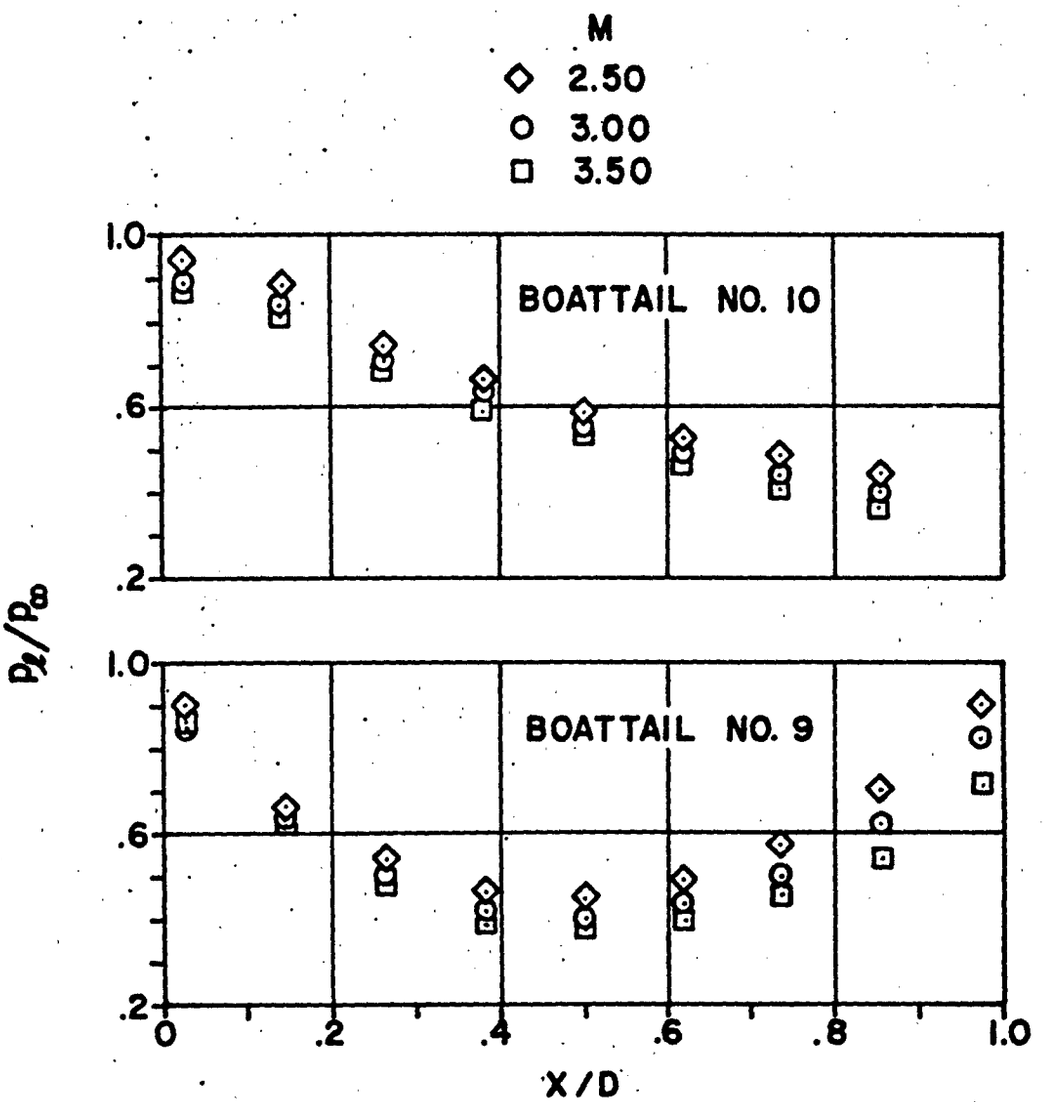

(d) Boattail Nos. 9 and 10

Figure 7. Continued

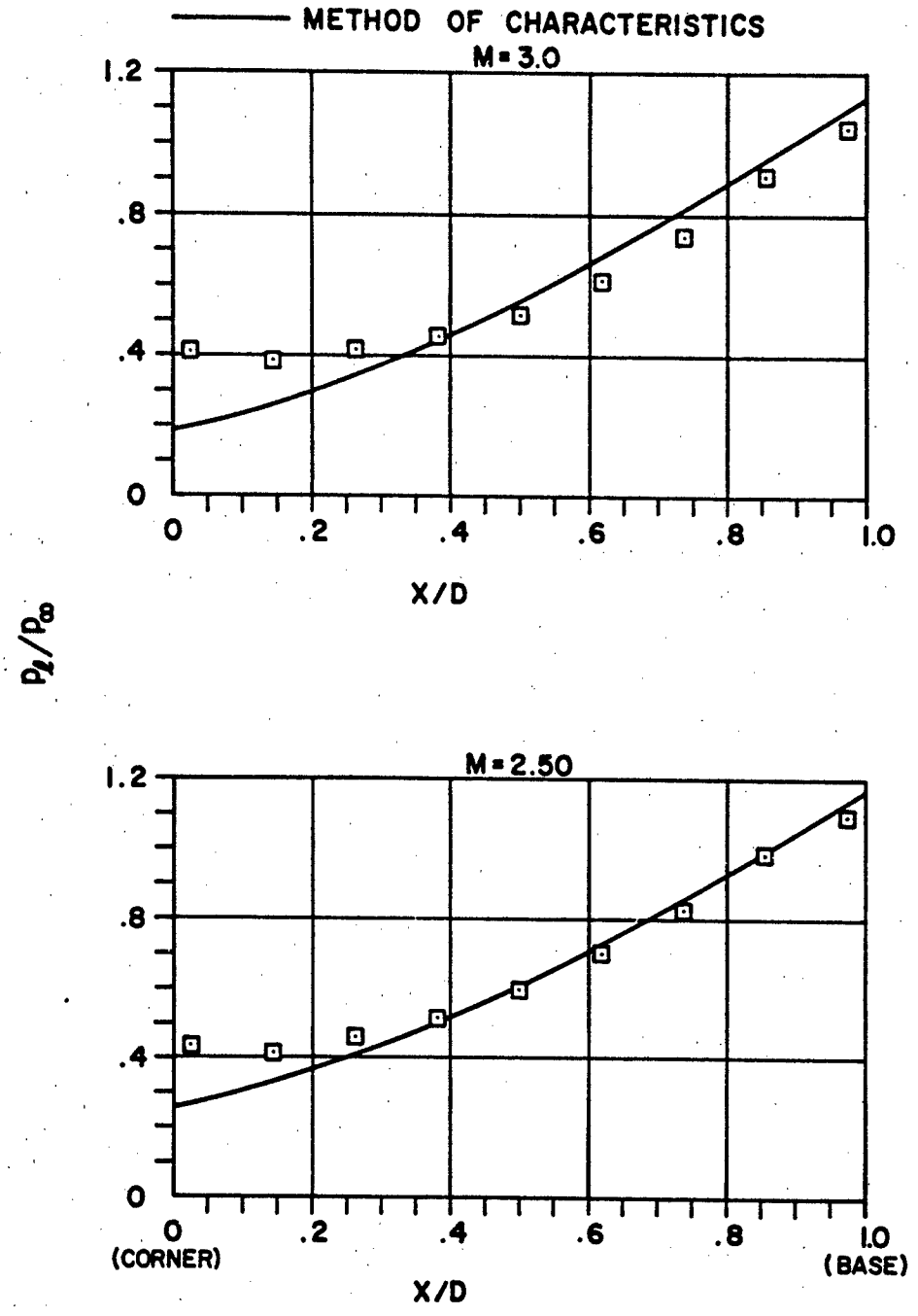

(e) Boattail No. 11

Figure 7. Concluded

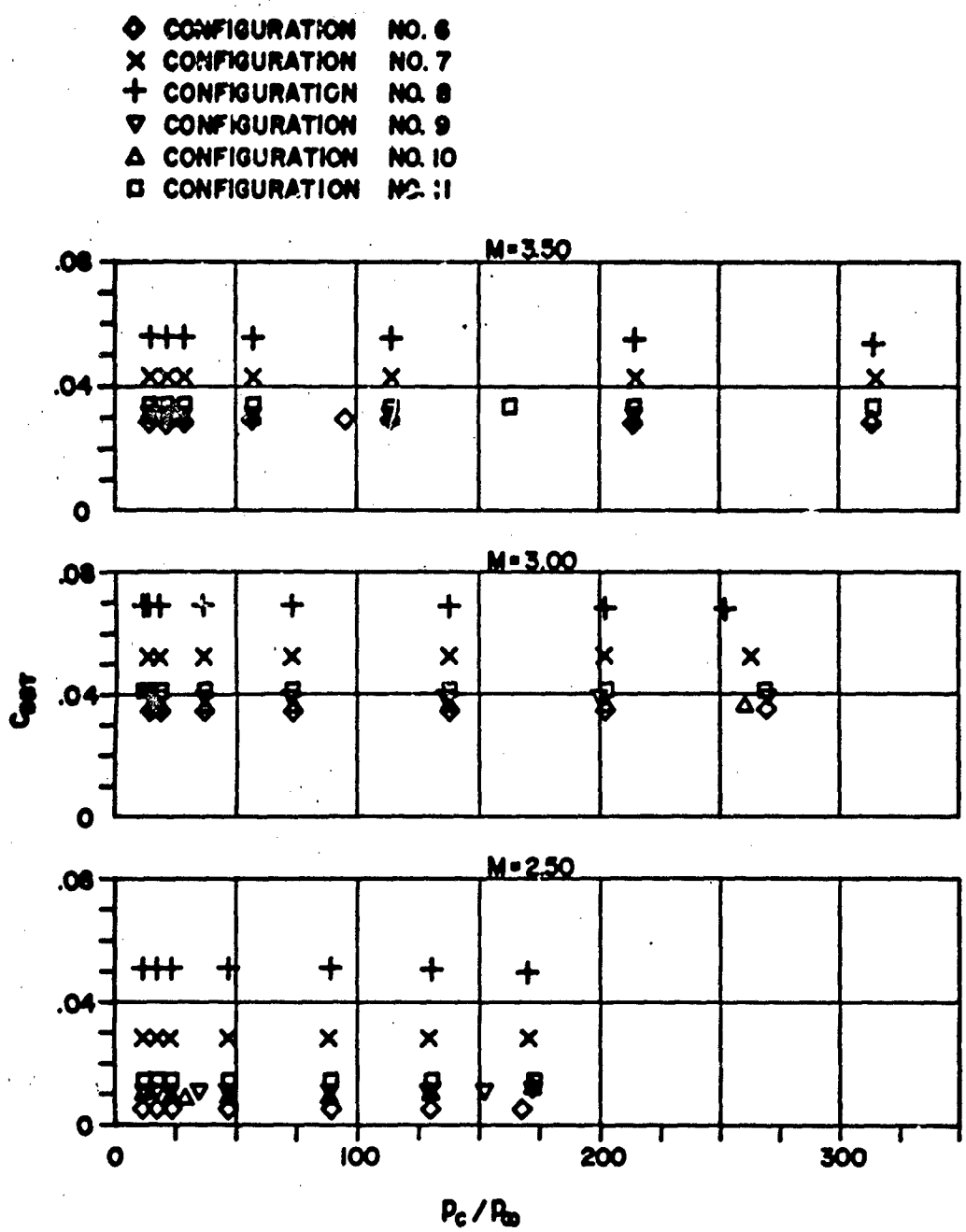

Figure 8. Effect of Sustainer Nozzle Operating Pressure on Boattail Drag

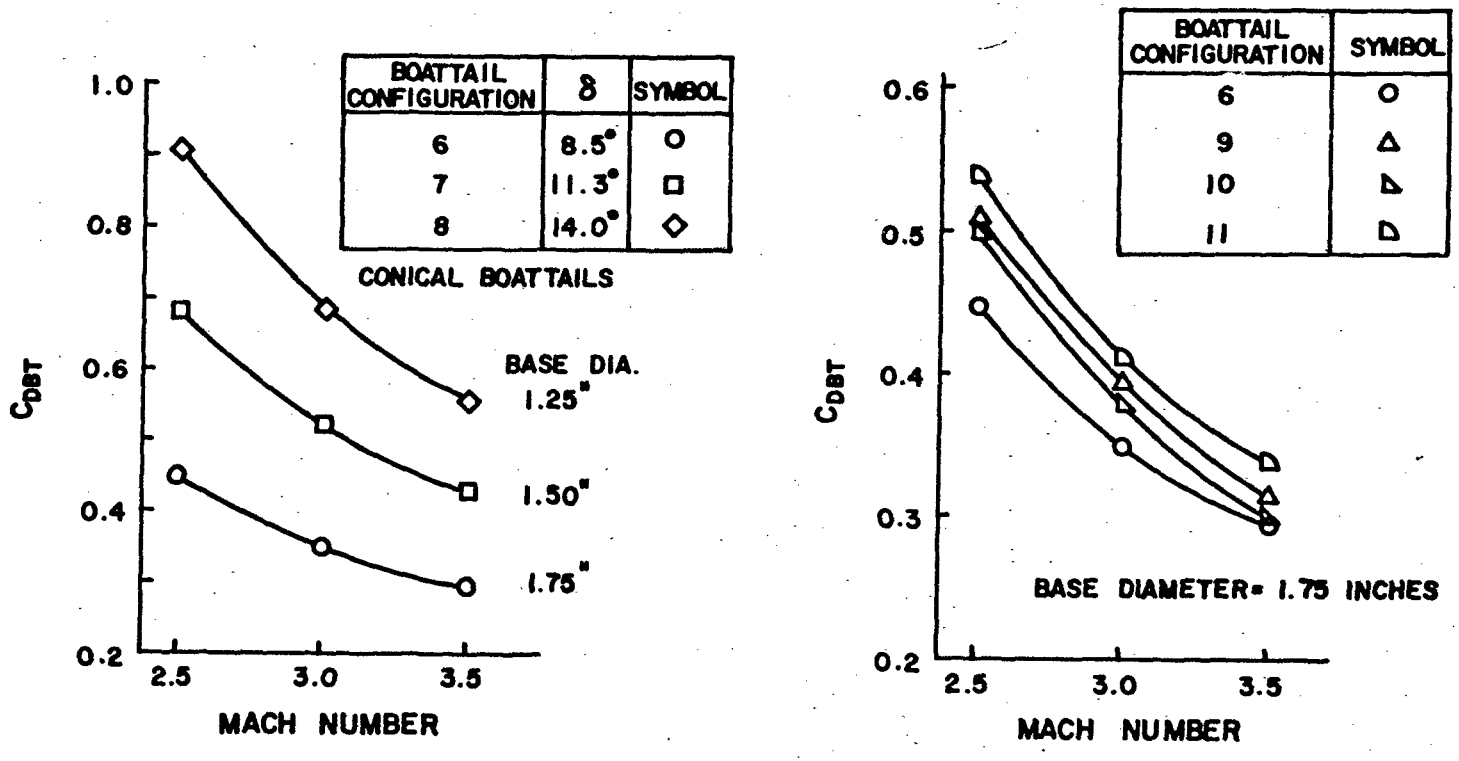

Figure 9. Effect of Mach Number on Boattail Drag

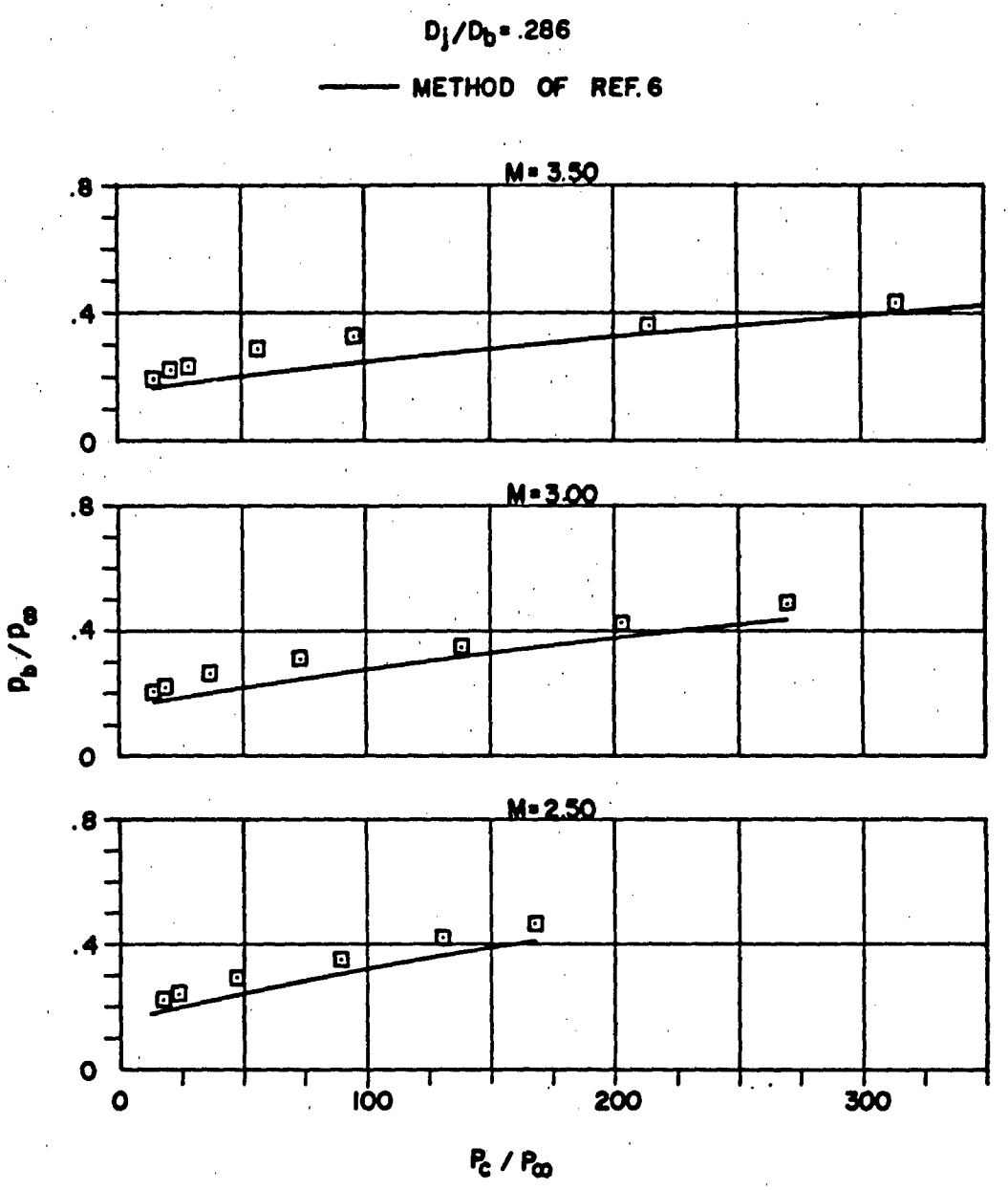

(a) Configuration No. 6

Figure 10. Effect of Sustainer Nozzle Operating Pressure on Base Pressure

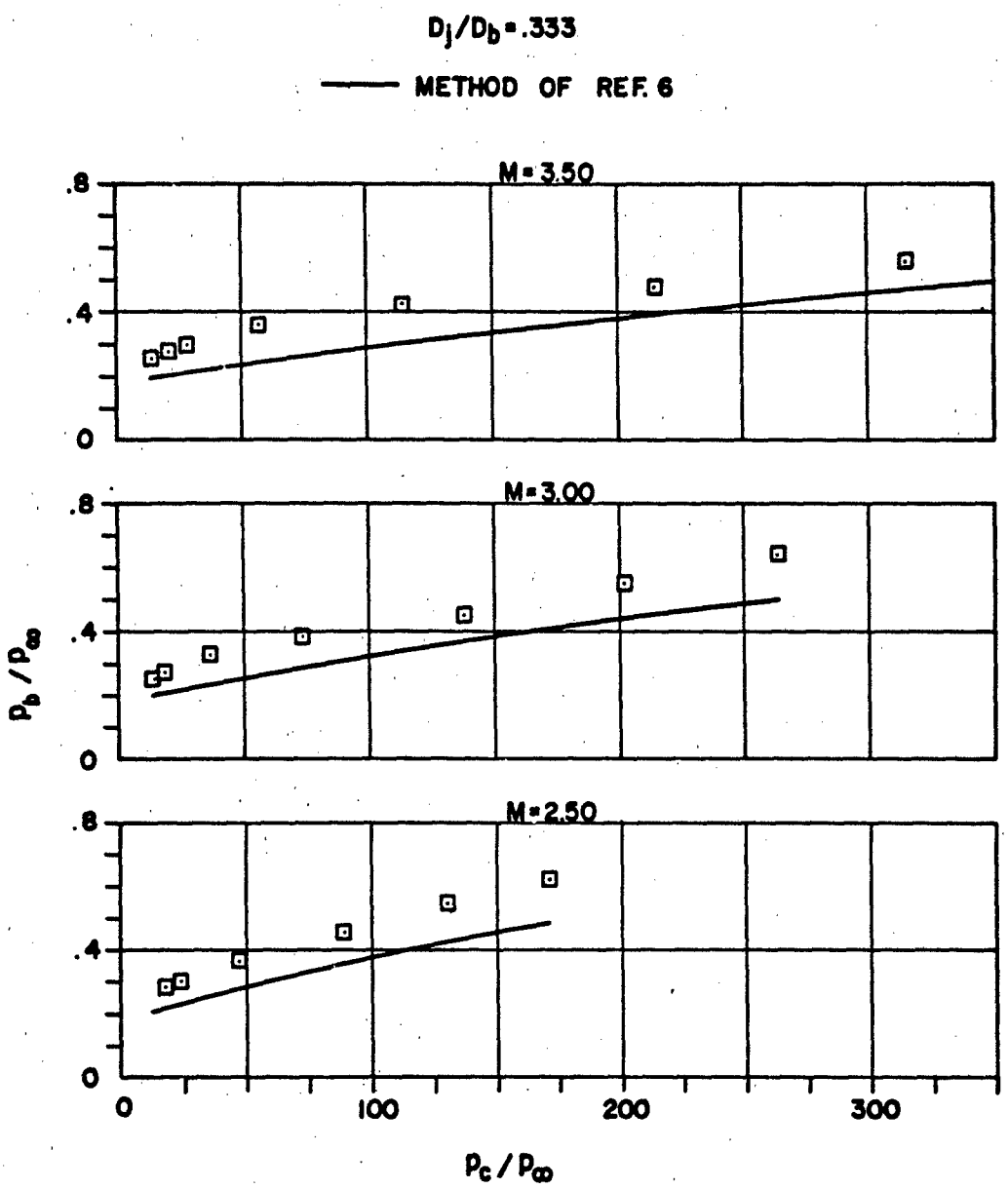

(b) Configuration No. 7

Figure 10. Continued

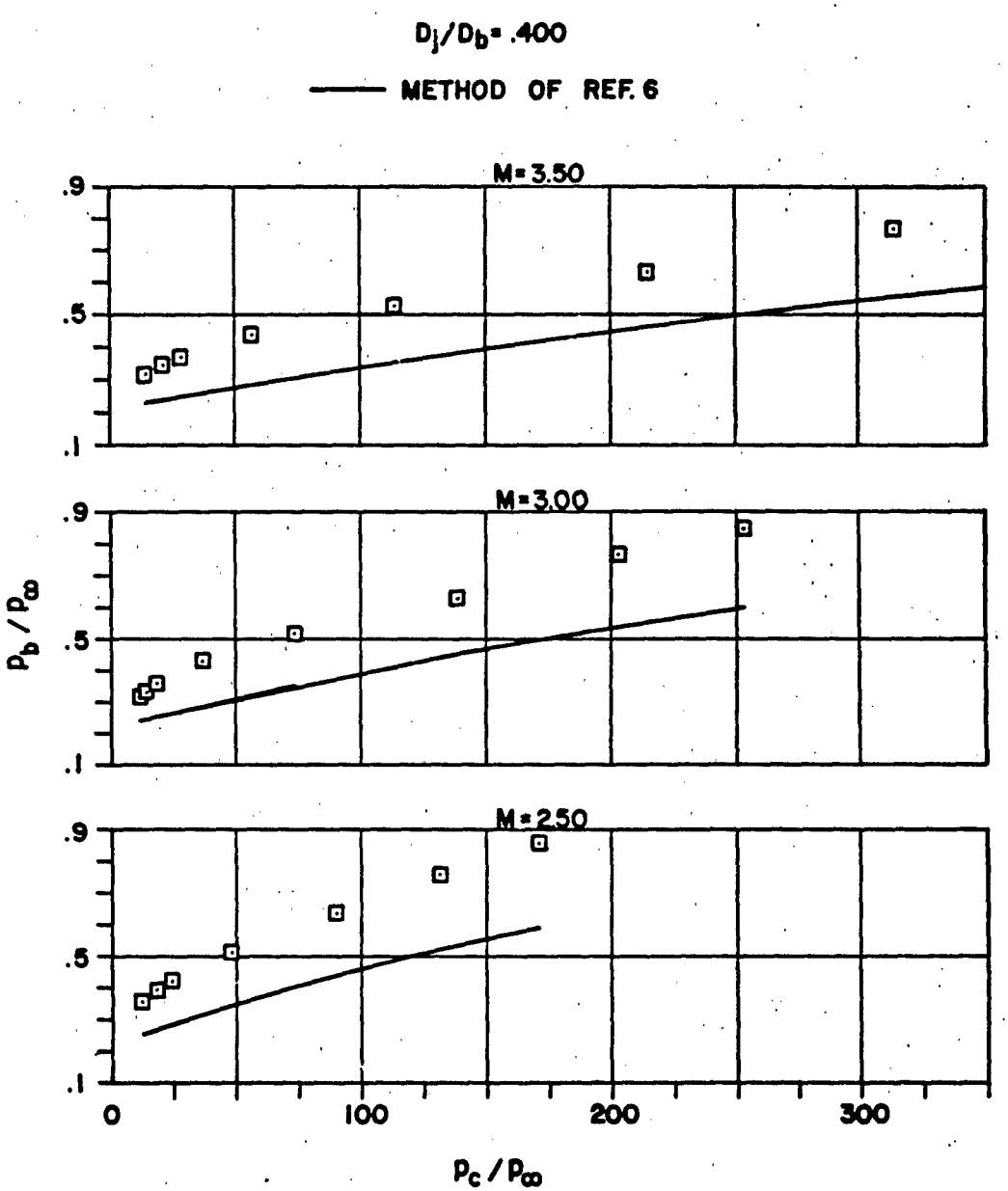

(c) Configuration No. 8

Figure 10. Concluded

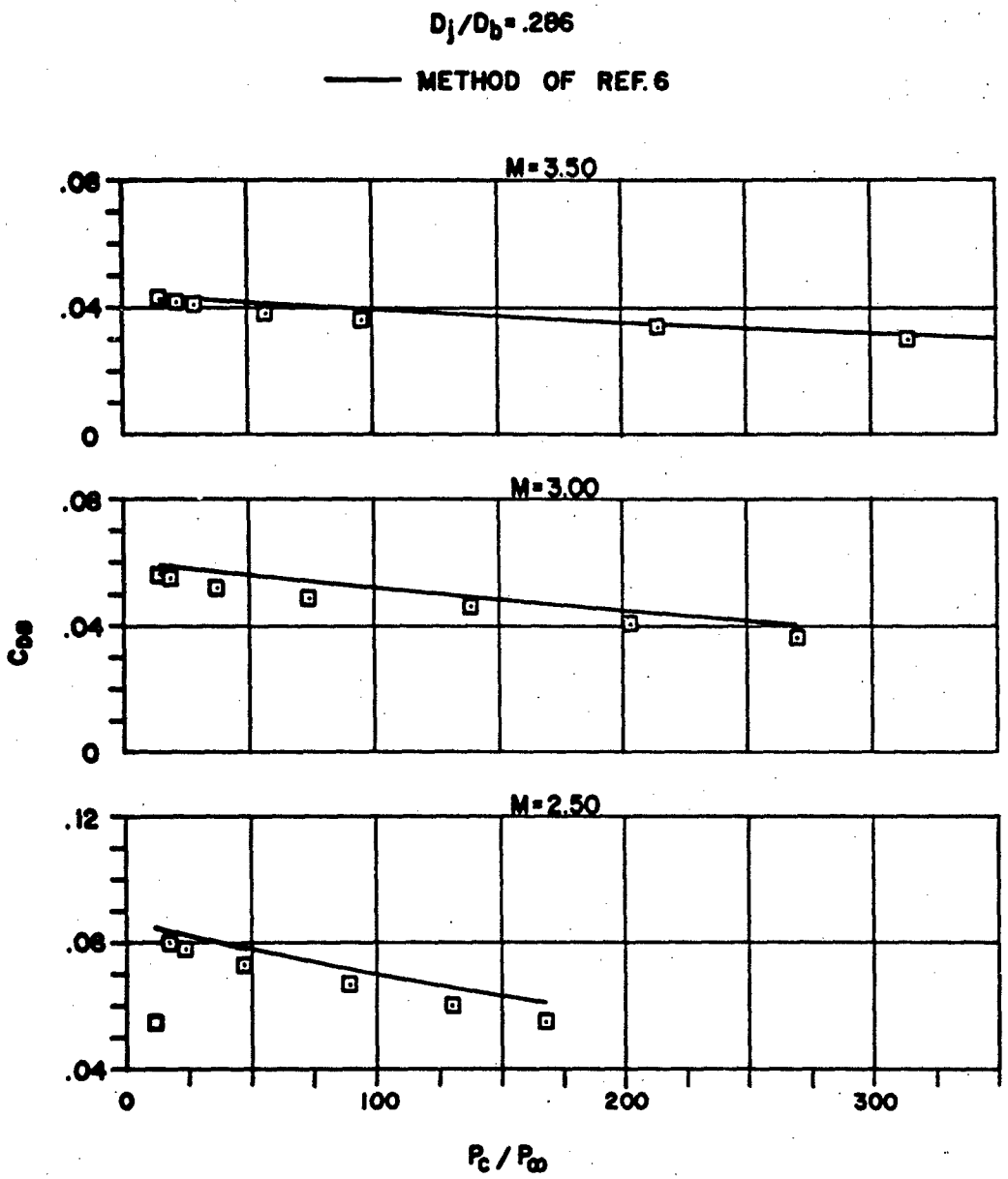

(a) Configuration No. 6

Figure 11. Effect of Sustainer Nozzle Operating Pressure on Base Drag

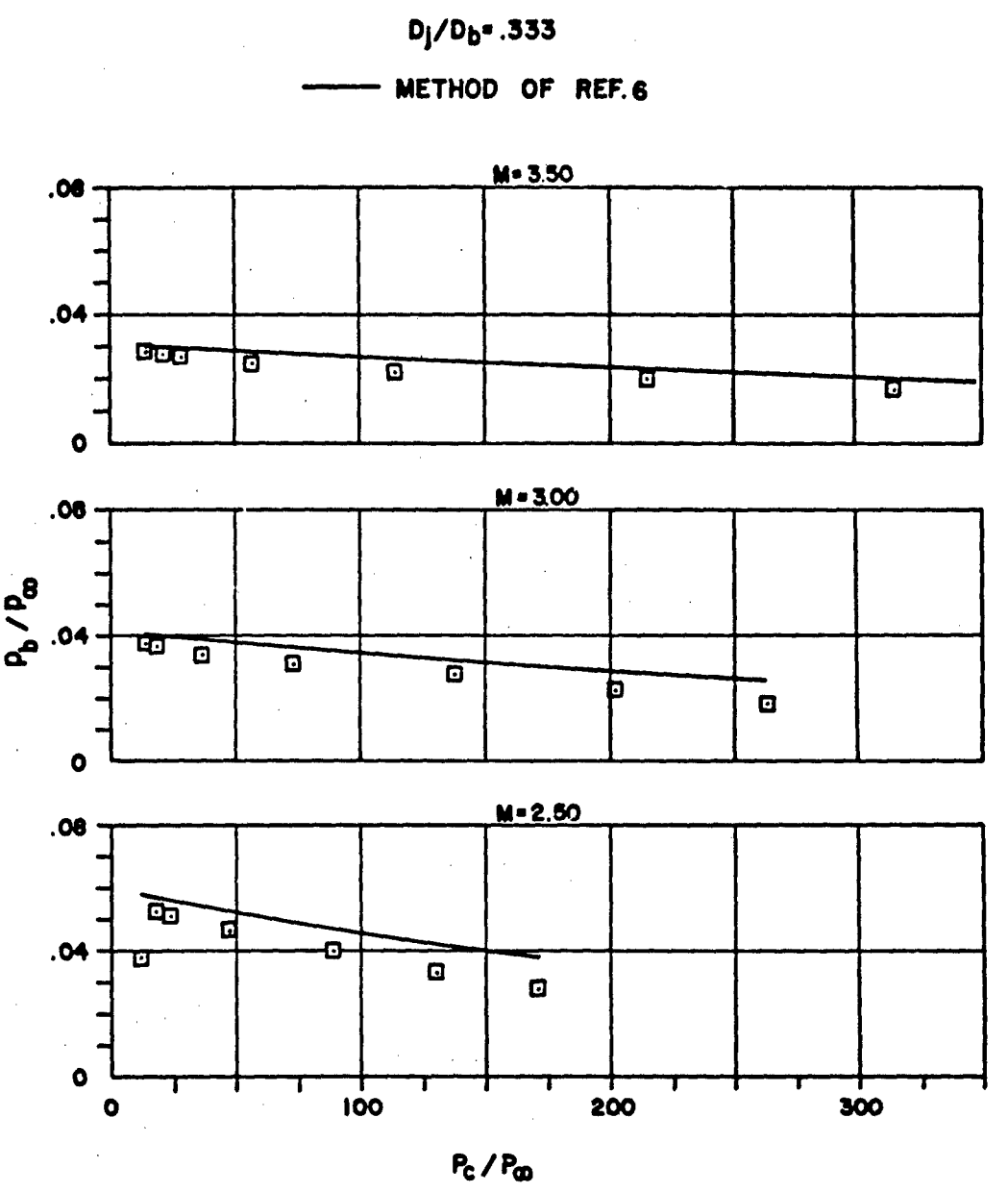

(b) Configuration No. 7

Figure 11. Continued

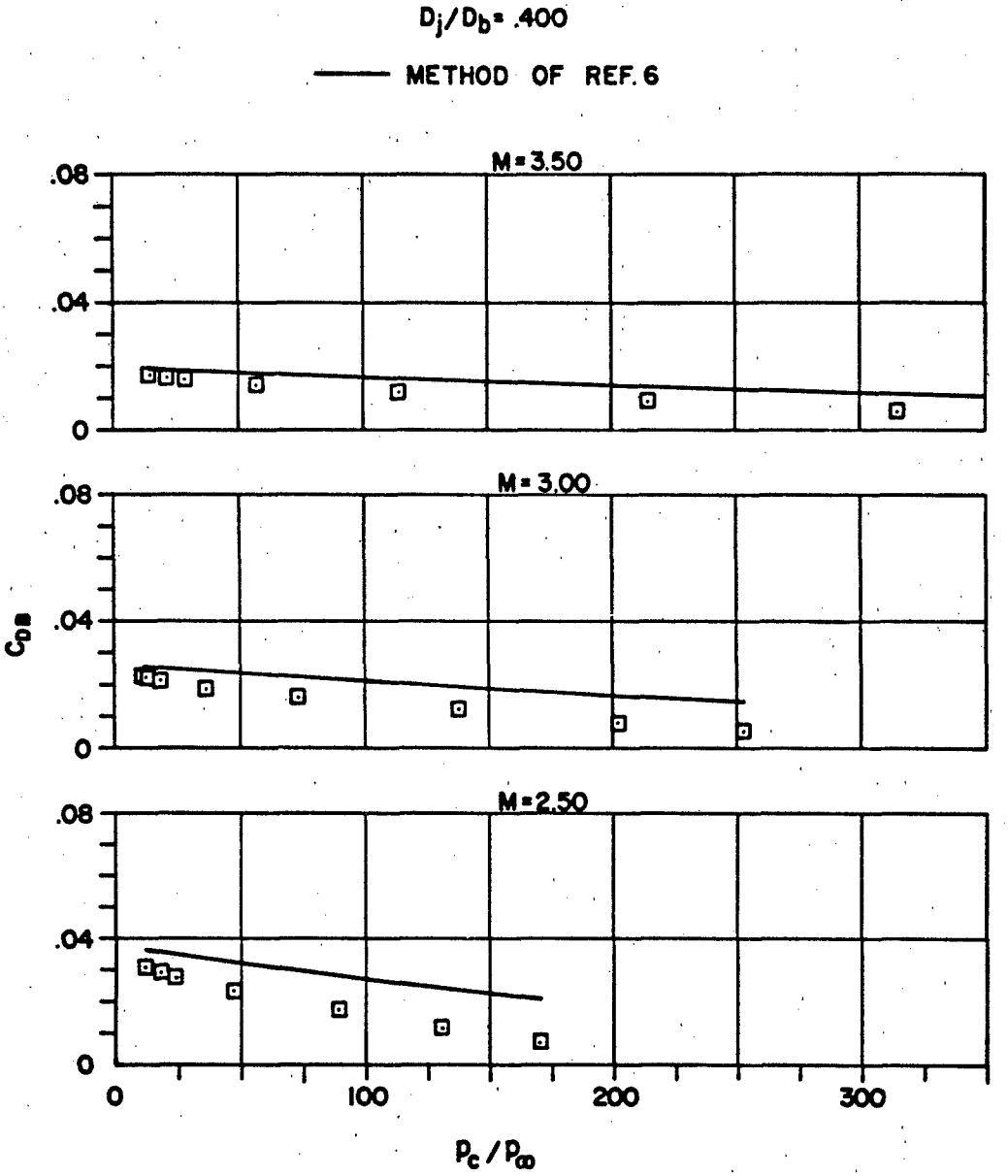

(c) Configuration No. 8

Figure 11. Concluded

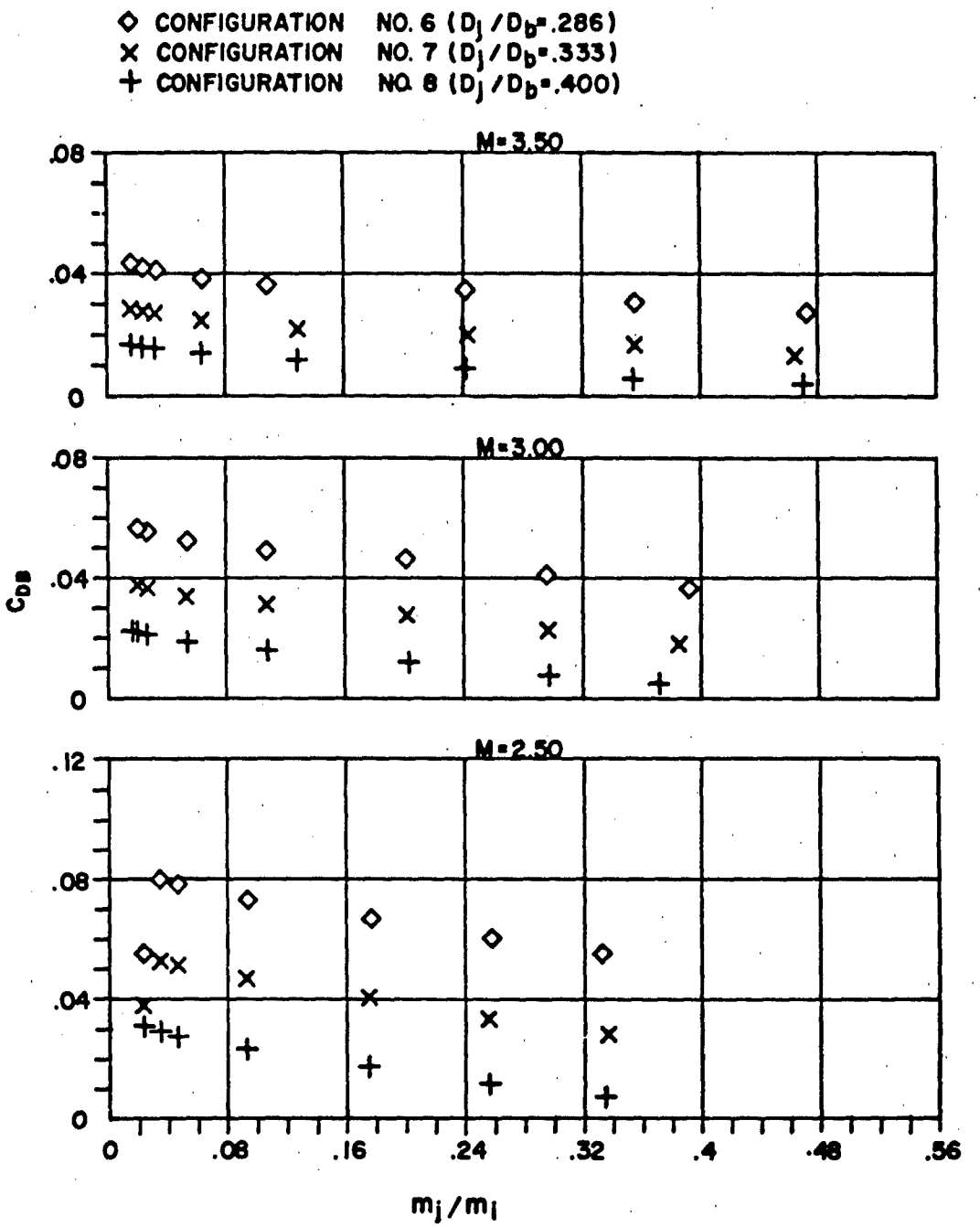

(a) Configuration Nos. 6, 7 and 8

Figure 12. Effect of Jet Mass Flow on Base Drag

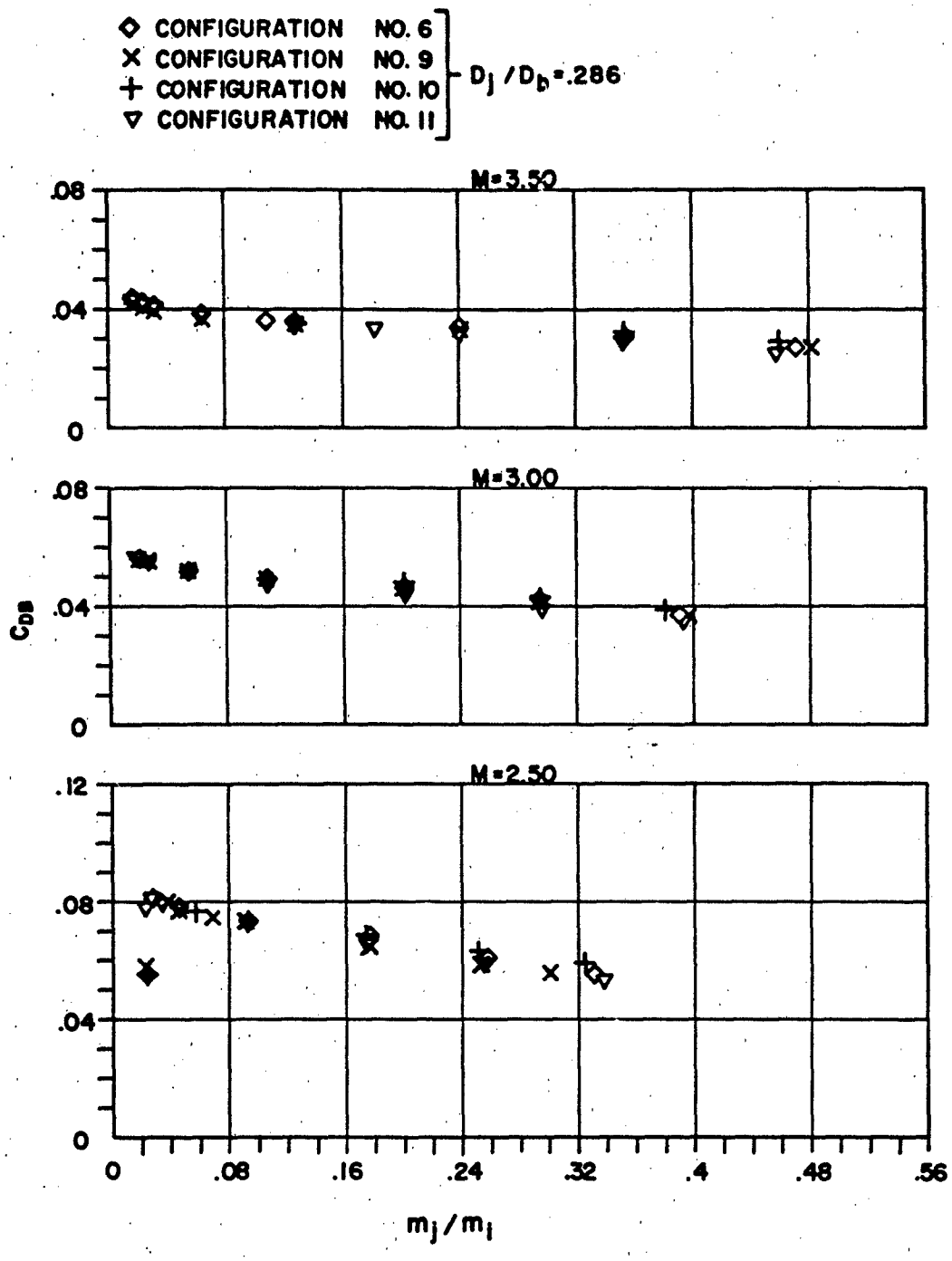

(b) Configuration Nos. 6, 9, 10 and 11

Figure 12. Concluded

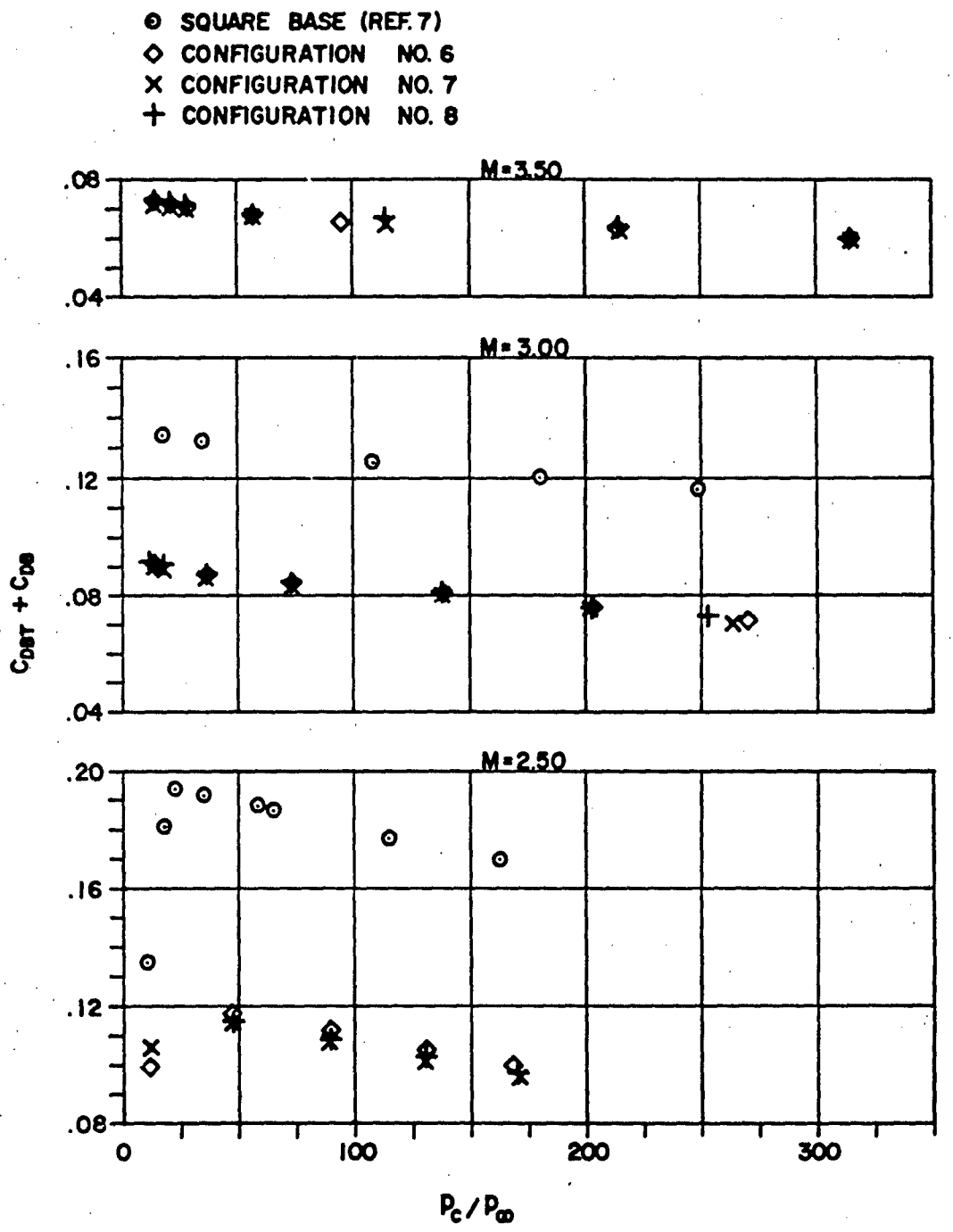

Figure 13. Effect of Sustainer Nozzle Operating Pressure on Total Drag

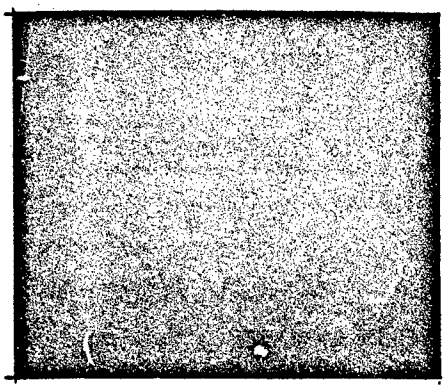

$P_c / P_\infty = 0$

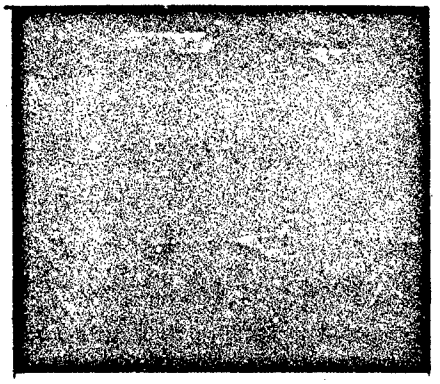

$P_c / P_\infty = 168$

M = 2.50

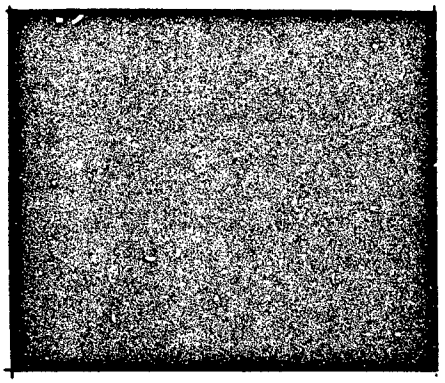

$P_c / P_\infty = 0$

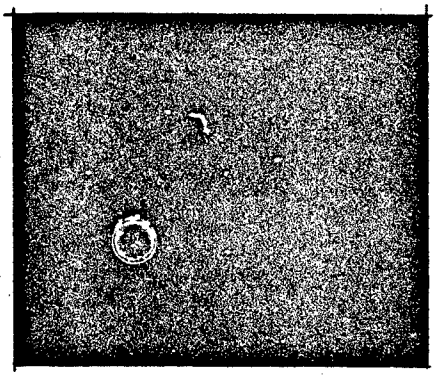

$P_c / P_\infty = 315$

M = 3.50

Figure 14. Schlieren Photographs of Base Flow Field for Boattail No. 6

REFERENCES

1. J. C. McMullen, "Wind Tunnel Testing Facilities at the Ballistic Research Laboratories," BRL Memorandum Report No. 1292, July 1960.

2. C. C. Bush, "Flow Characteristics of the Ballistic Research Laboratories' Supersonic Wind Tunnel No. 1," BRL Memorandum Report No. 1731, February 1966.

3. R. Colburn, "Pressure Scanner Unit," BRL Technical Note No. 1616, June 1966.

4. Ames Research Staff, "Equations, Tables and Charts for Compressible Flow," NACA Report No. 1135, 1953.

5. C. A. Syvertson and D. H. Dennis, "A Second-Order Shock-Expansion Method Applicable to Bodies of Revolution Near Zero Lift," NACA Report No. 1328, 1957.

6. C. E. Brazzel and J. H. Henderson, "A Correlation of the Base Drag of Bodies of Revolution With a Jet Exhausting Through the Base," Paper presented at Army Science Conference, 1966.

7. J. Huerta, "The Effect of Rocket Nozzle Geometry and Secondary Flow Field on Base Drag at Mach Numbers 2.50 and 3.00, An Experimental Investigation," BRL Memorandum Report No. 1829, March 1967.

Unclassified
Security Classification

DOCUMENT CONTROL DATA - R & D

(Security classification of title, body of abstract and indexing annotation must be entered when the overall report is classified)

1. ORIGINATING ACTIVITY (Corporate author) U.S. Army Aberdeen Research and Development Center Ballistic Research Laboratories Aberdeen Proving Ground, Maryland	2a. REPORT SECURITY CLASSIFICATION Unclassified 2b. GROUP

3. REPORT TITLE

AN EXPERIMENTAL INVESTIGATION AT SUPERSONIC MACH NUMBERS OF BASE DRAG OF VARIOUS BOATTAIL SHAPES WITH SIMULATED BASE ROCKET EXHAUST

4. DESCRIPTIVE NOTES (Type of report and inclusive dates)

5. AUTHOR(S) (First name, middle initial, last name)

Joseph Huerta

6. REPORT DATE	7a. TOTAL NO. OF PAGES	7b. NO. OF REFS
June 1969	46	7

8a. CONTRACT OR GRANT NO.	9a. ORIGINATOR'S REPORT NUMBER(S)
b. PROJECT NO. RDT&E Project No. 1T061102A33D	Memorandum Report No. 1983
c.	9b. OTHER REPORT NO(S) (Any other numbers that may be assigned this report)
d.	

10. DISTRIBUTION STATEMENT

This document is subject to special export controls and each transmittal to foreign governments or foreign nationals may be made only with prior approval of Commanding Officer, U.S. Army Aberdeen Research and Development Center, Aberdeen Proving Ground, Maryland.

11. SUPPLEMENTARY NOTES	12. SPONSORING MILITARY ACTIVITY
	U.S. Army Materiel Command Washington, D.C.

13. ABSTRACT

An experimental investigation was conducted to determine the effect of boattail geometry and simulated base rocket nozzle flow on overall base drag. All tests were performed at Mach numbers 2.50, 3.00 and 3.50. Reasonable prediction of base drag for the reported boattail shapes can be made by using approximate and empirical equations. A conical boattail produced less drag than the other boattail shapes investigated. The maximum nozzle stagnation to free-stream pressure ratio reported is 315.

DD FORM 1 NOV 68 1473 REPLACES DD FORM 1473, 1 JAN 64, WHICH IS OBSOLETE FOR ARMY USE.

Unclassified
Security Classification

14. KEY WORDS	LINK A		LINK B		LINK C	
	ROLE	WT	ROLE	WT	ROLE	WT
Supersonic Flow						
Base Drag						
Base Rocket						
Boattail Drag						
Base Pressure						
Boattail Pressure						